

Mobility of Spin Probes in Nylon Films. 1. Nonionic Spin Probes

Kunihiro Hamada and Toshiro Iijima*

Department of Polymer Science, Tokyo Institute of Technology, Ookayama, Meguro-ku, Tokyo 152, Japan

Ralph McGregor

Department of Textile Chemistry, North Carolina State University, Raleigh, North Carolina 27695-8302. Received September 4, 1985

ABSTRACT: The mobility of nonionic spin probes in nylon films was investigated by electron spin resonance (ESR). Dried samples were used to avoid the effects of water in the polymer matrices. Effects of drawing were observed only for spin probes having an amino or amide group, suggesting that the orientation of the nylon chain molecules affects the interaction of these spin probes with the macromolecules. T_{50G} , the temperature at which the extrema separation of the ESR spectra becomes 5 mT (50 G), decreased with increasing methylene chain length of the nylon. In other words, the longer the methylene chain, the larger the mobility of the spin probes. In the Arrhenius plots of rotational correlation times one or two crossover points were defined. The number of crossover points was found to vary from probe to probe. For probe molecules carrying substituent groups linked by single bonds two crossover points could be defined. The crossover point at the lower temperature, T_n' , is presumed to be the temperature at which rotation around the single bond occurs, and that at the higher temperature, T_n , is considered to be the temperature at which rotational motion of the whole probe molecule takes place. The dependence of the activation energy for rotation, in the temperature region above T_n , on the methylene chain length of the nylon is influenced by the interaction of the probe molecules with the nylons and by the jumping distance of the spin probes.

Introduction

The mobility of small molecules in polymer matrices is of interest in the broad area of polymer science. The permeation of ions through membranes and the dyeing of fibers are pertinent examples. In recent years the permselectivity of synthetic polymer membranes has been an important research subject and the study of the mobility of small molecules in films has become more and more important. This problem is also a matter of interest in the field of biochemistry.

In the present work the mobilities of nonionic spin probes in nylon films were investigated by electron spin resonance (ESR) measurements. The ESR spin probe technique has been widely used for solid polymers, polymer solutions, bilayers, and micelles.^{1,2} Previous work on solid polymers has provided useful information on the mobility of a spin probe in a solid macromolecular medium. Kumler et al.^{3,4} and Törmälä et al.^{5,6} discussed the correlation of the glass transition temperature, T_g , with T_{50G} , the temperature at which the extrema separation becomes 5 mT (50 G). Kusumoto et al.⁷ and Bullock et al.⁸ interpreted these relations by means of Bueche's free volume theory⁹ and evaluated the segmental volume of the polymer concerned in the motions. In these analyses, however, the interactions between probe molecules and macromolecules have not been considered.

The effects of changes in polymer structure, e.g., in the drawing of polyethylene film^{10,11} and polypropylene film,¹² and in the acylation of chitin films¹³ and poly(*O*-acyl-hydroxy-L-proline) films¹⁴ were investigated with respect to the mobility of spin probes. However, there are no spin probe investigations to make clear the effects of the methylene groups of a polymer main chain on the mobility of spin probes.

Törmälä et al.^{15,16} studied the effects of water on the mobility of a spin probe in a nylon fiber qualitatively. In our previous work¹⁷ on nonionic spin probes in nylon 6 film in the presence of water, we discussed quantitatively the effects of water on the mobility and then considered the interaction between the nylons and the probe molecules.

As an extension of this work, in the present study the effects of drawing, of the methylene chain length of the nylon films, and of the spin probe structures are discussed, taking into account the interactions between the nylons and the probe molecules. All of the samples measured were dried to avoid the effects of water.

Experimental Section

The three nonionic spin probes shown in Figure 1 were used. Their preparation was described in our previous paper.¹⁸ Five nylon films were used. Undrawn nylon 4 film (NY-4) was prepared by casting from formic acid solution of nylon 4 powder synthesized by a conventional method. Biaxially drawn nylon 6 film (NY-6(2D)) and undrawn nylon 6 film (NY-6(ND)) were kindly supplied by Unitika Co. Nylon 11 film (NY-11) and nylon 12 film (NY-12), both drawn by inflation, were cordially supplied by Daicell Co. The physical structures were stabilized and water-soluble oligomers were removed by pretreating all the films in boiling water for 3 hours.

The spin probes were sorbed by the nylon films from aqueous solution at 373 K for 1 h. The amounts of the probes sorbed were calculated by determining spectrophotometrically the initial and final bath concentrations. The amounts sorbed were at the same level for all nylon films and spin probes, i.e., $(1-5) \times 10^{-6}$ mol/g of the nylon. After sorption, the film was rinsed with cold water, blotted with filter paper, and dried in vacuo at 393 K for 1 day. The film thus prepared was put into an ESR tube and sealed in the presence of air.

ESR spectra were obtained with a JEOL-FE3X ESR spectrometer in the X band. The modulation width and the microwave power were kept at 0.1 mT and 0.4 mW, respectively, to avoid line broadening and saturation effects. The temperature was changed from 130 to 465 K by using a JES-VT-3A2 variable-temperature controller together with a JES-UCT-2AX variable-temperature adapter.

Results and Discussion

Extrema Separation. Examples of ESR spectra are shown in Figure 2. The extrema separation $2A_z'$ reflects the mobility of spin probes and decreases with an increase of the mobility. As shown in Figures 3-5, $2A_z'$ decreased with increasing temperature. However, the dependence of $2A_z'$ on temperature varies from probe to probe. $2A_z'$

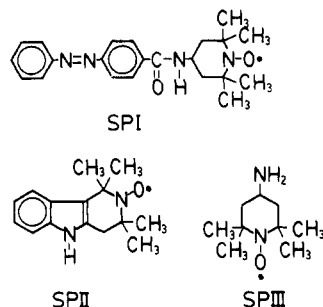


Figure 1. Spin probes used.

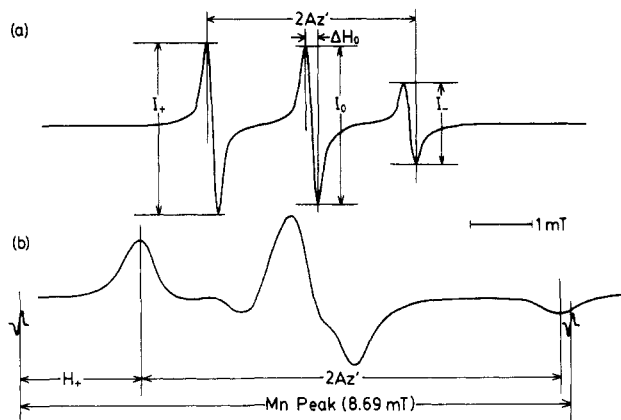
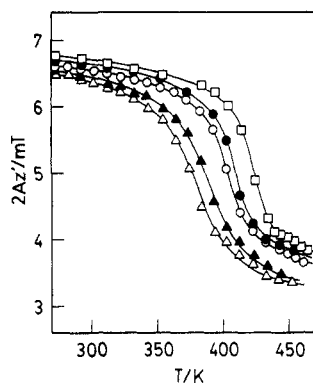
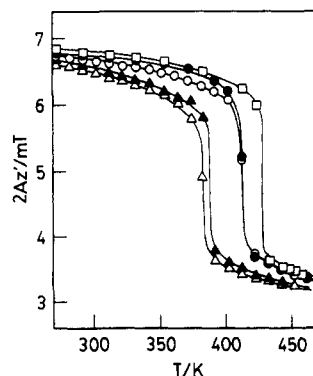
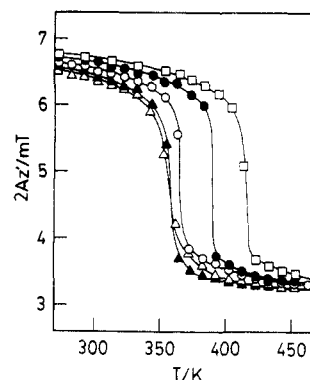


Figure 2. ESR spectra of SPIII in NY-12: (a) 423 K; (b) 221 K.

Figure 3. $2Az'$ vs. temperature. SPI. (\square) NY-4; (\bullet) NY-6(2D); (\circ) NY-6(ND); (\blacktriangle) NY-11; (\triangle) NY-12.Figure 4. $2Az'$ vs. temperature. SPII. (\square) NY-4; (\bullet) NY-6(2D); (\circ) NY-6(ND); (\blacktriangle) NY-11; (\triangle) NY-12.

for SPI, 4-((*p*-phenylazobenzoyl)amino)-2,2,6,6-tetramethylpiperidinoxy, changed more gently with temperature than for SPII and SPIII. The shape of the curve also varies from nylon to nylon. For SPI, the change became

Figure 5. $2Az'$ vs. temperature. SPIII. (\square) NY-4; (\bullet) NY-6(2D); (\circ) NY-6(ND); (\blacktriangle) NY-11; (\triangle) NY-12.Table I
 T_{50G} , T_n' , and T_n (K)

	NY-4	NY-6(2D)	NY-6(ND)	NY-11	NY-12
SPI					
T_{50G}	424	408	404	388	376
T_n'	381	371	362	354	336
T_n	441	423	425	403	389
SPII					
T_{50G}	428	414	414	388	385
T_n	412	394	399	383	374
SPIII					
T_{50G}	416	391	365	360	354
T_n'	366	365	347	333	332
T_n			403	379	380

more gentle with increasing methylene chain length of the nylon. The curves for SPII and SPIII had no such tendency. The effects of drawing increased in the order SPII < SPI < SPIII, which was evaluated in terms of the difference of $2Az'$ between the drawn and undrawn films, and were more pronounced in the lower temperature region for all cases. As the mobility should change for different medium and probe molecules, the shapes of the curves can be expected to vary from system to system. Kumler et al.⁴ correlated the shapes of the curves to the physical properties of the polymers, i.e., "sharp" curves to polymers with low T_g 's (e.g., poly(dimethylsiloxane)) and "diffuse" curves to polymers with high T_g 's (e.g., polycarbonate). This argument is, however, based only on the results for a single hydrophobic spin probe and may not be valid in general. In fact the shapes of the curves probably reflect the interactions of the probe molecules with the macromolecules, as well as the rotation of the probe molecules. As the shape is determined by the change of the rotational correlation time τ_R with temperature, the detailed discussion is given in the next section.

T_{50G} , at which $2Az'$ becomes 5 mT (50 G), is shown in Table I. T_{50G} decreased in the order NY-4 > NY-6(2D) \geq NY-6(ND) > NY-11 > NY-12. Kumler et al.^{3,4} and Törmälä et al.^{5,6} found the correlation between T_{50G} and T_g experimentally. The former authors, however, estimated the correlation on the basis of the results for only one hydrophobic spin probe as mentioned before. On the other hand, the latter authors did not consider the interactions between macromolecules and probe molecules. Kusumoto et al.⁷ and Bullock et al.⁸ also gave the correlation without considering the interaction effects. Hlousková et al.¹⁹ estimated the effective free volume of spin probes in cross-linked isotactic polypropylene by considering the structures of the probe molecules. The discrepancies in the free volumes determined by the methods of Kusumoto et al.⁷ and Bullock et al.⁸ for dif-

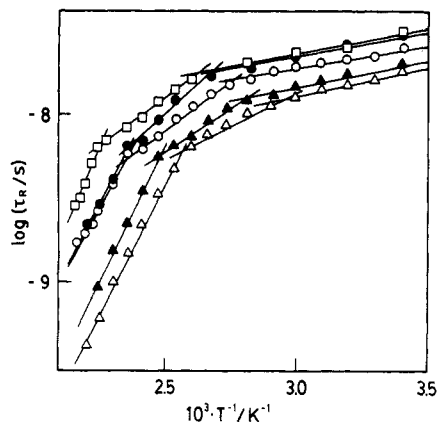


Figure 6. Arrhenius plots of τ_R . SPI. (\square) NY-4; (\bullet) NY-6(2D); (\circ) NY-6(ND); (\blacktriangle) NY-11; (\triangle) NY-12.

ferent spin probes presumably reflect the nonrigid character of the probe molecules, as well as the shapes of the free volume regions in which the motions of the probe molecules take place. However, our results cannot be explained by the above argument. T_g values for NY-4, NY-6(2D), NY-6(ND), NY-11, and NY-12 were determined as 373, 358, 318, 340, and 331 K, respectively, by means of dynamic mechanical measurement at 10 Hz. These values are inconsistent with the T_{50G} values. An essential problem here is the difference in the physical meanings of T_g and T_{50G} . T_g reflects the macroscopic character of the segmental mobility of polymers, while T_{50G} gives purely microscopic information through the mobility of spin probes. Some of the differences found between T_g and T_{50G} are believed to reflect different effective frequencies of measurement.²⁰ The drawing of a film influences T_g in a definite way, while the effect on T_{50G} varies from probe to probe. As T_{50G} obviously reflects the microenvironment around the probe molecule, the interaction between macromolecules and probe molecules should be considered as suggested by Bullock et al.⁸ and Buchachenko et al.²¹

Rotational Correlation Times. Rotational correlation times τ_R were determined from the spectra obtained. τ_R in the region from 1×10^{-11} to 5×10^{-9} s was calculated from eq 1 derived by Kivelson.²² In eq 1 $R_{\pm} = (I_0/I_{\pm})^{1/2}$,

$$\tau_R = (6.64 \times 10^{-10}) \Delta H_0 (R_+ + R_- - 2) \quad (1)$$

I_+ , I_0 , and I_- are the amplitudes of the peaks at low, center, and high field, respectively, and ΔH_0 is the line width of the center peak (see Figure 2). τ_R in the region from 5×10^{-9} to 1×10^{-7} s was determined by means of eq 2 derived

$$\kappa = \frac{H_+ - H_{(\tau_R \rightarrow 0)}}{H_{+(\tau_R \rightarrow \infty)} - H_{+(\tau_R \rightarrow 0)}} \quad (2)$$

by Kuznetsov et al.²³ In eq 2 κ is a parameter with a one-to-one correspondence to τ_R , and H_+ is the position of the low-field derivative line (see Figure 2). The value obtained for NY-4 at 130 K was used as $H_{+(\tau_R \rightarrow \infty)}$, the reference value in the rigid state. The value in solution was used as the limiting value $H_{+(\tau_R \rightarrow 0)}$ for free rotation. τ_R used here was determined with the assumption of isotropic rotation, and it should be termed the "apparent rotational correlation time". A more detailed discussion of τ_R can be found in our previous paper.¹⁸

The Arrhenius plots of τ_R are shown in Figures 6–8. For SPI, two distinct crossover points were defined, but only one could be clearly defined for SPII. SPIII had a different number of crossover points for different nylons. It was concluded that NY-4 and NY-6(2D) have only one, while NY-6(ND), NY-11, and NY-12 have two distinct crossover

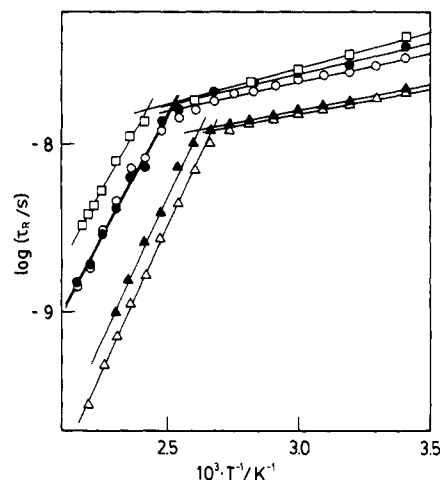


Figure 7. Arrhenius plots of τ_R . SPII. (\square) NY-4; (\bullet) NY-6(2D); (\circ) NY-6(ND); (\blacktriangle) NY-11; (\triangle) NY-12.

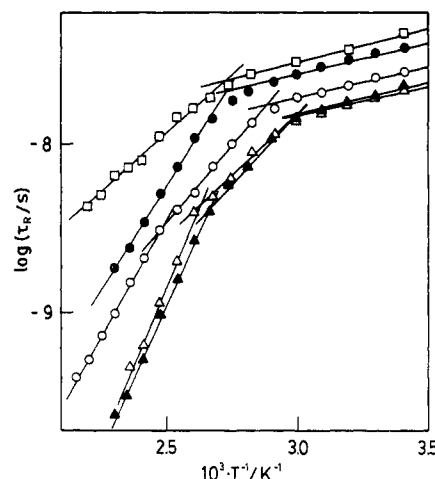


Figure 8. Arrhenius plots of τ_R . SPIII. (\square) NY-4; (\bullet) NY-6(2D); (\circ) NY-6(ND); (\blacktriangle) NY-11; (\triangle) NY-12.

points in the temperature range investigated. The crossover point in the low-temperature region for SPI and SPIII is designated as T_n' and that in the high-temperature region as T_n . The crossover point for SPII is also designated as T_n . The existence of two crossover points may be explained as follows. In the case of SPI, rotation around the single bond linking the probe moiety to the NH group probably occurs. Rotation around other single bonds hardly takes place owing to the resonance of the π -orbitals. The temperature at which this single-bond rotation occurs is assumed to correspond to T_n' for SPI. SPIII would probably be bound to the nylon chains through hydrogen bonds. The temperature at which the rotation around a $>C-NH_2$ single bond occurs is assumed to correspond to T_n' for SPIII. On the other hand, T_n is probably the temperature at which the rotational motion of the whole molecule takes place: above T_n the spin probe rotates without any restriction from specific bonding to the macromolecule. T_n' and T_n are shown in Table I. Both T_n' and T_n decreased with increasing methylene chain length; i.e., the mobility increased with the number of methylene groups. T_n was not influenced by drawing, but T_n' was different for NY-6(2D) and NY-6(ND). The largest effect of drawing on the mobility was found for SPIII. It is thought that the interaction between SPIII and the chain molecules varies from nylon to nylon. Three modes of interaction, as shown in Figure 9, are considered possible. The orientation of the chain molecules in the drawn nylon film makes it easier for SPIII to interact with

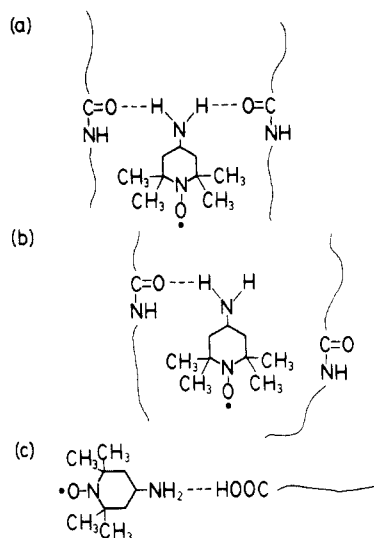


Figure 9. Model of the interaction between SPIII and the nylon chain.

the nylon chain through two hydrogen bonds (Figure 9a). As a result of such an interaction, the rotation would be more severely hindered. In the undrawn film SPIII may interact either with the amide groups or with the end groups (Figure 9b,c), and rotation should be easier. As Table I shows, T_n for SPIII is similar to that for SPII, so that the T_n values cannot be explained only in terms of the relative molar volumes. This fact clearly indicates that Kusumoto's argument⁷ is not correct, in which T_n increases with increasing molar volume of the spin probe. As mentioned above, SPIII is believed to be bound to the nylon chain through hydrogen bonds, and these bonds must be broken if the rotation of the whole probe molecule is to occur, which results in an increase of T_n . In this context we can conclude that T_n reflects the effect of both the molar volume and the specific interactions between the probe molecule and the macromolecule.

For further discussion, the activation energies for rotation E_a^R were determined from Figures 6–8 and are given in Table II. Although τ_R values below 293 K are not shown in the figures, they were used to determine E_a^R in the low-temperature region. E_a^R in the temperature region below T_n' (for SPII, below T_n) ("low") was similar for all the systems. The spin probes probably undergo rotational vibrations only in this region, owing to the difficulty of the motion of the polymer chain. E_a^R in this region is also only a few $\text{kJ}\cdot\text{mol}^{-1}$ for other polymer/spin probe systems²⁴ and thus does not vary significantly with the system. In the temperature region between T_n' and T_n ("medium") there is some tendency for E_a^R for drawn samples to increase with a decrease in the methylene chain length. This presumably reflects interactions between the probe molecule and the nylon chain. As shown in Figure 9, the mode of hydrogen bond formation might vary in different nylons. Orientation of the nylon chain would facilitate hydrogen bonding as in Figure 9a, leading to difficulty of rotation. The data for NY-6(2D) show the largest activation energy, consistent with bonding as in Figure 9a, while NY-6(ND), NY-11, and NY-12 may have the interaction modes of Figure 9b,c. On the other hand, NY-4 has a higher concentration of amide groups than the other nylons and so might easily form hydrogen bonds of the type shown in Figure 9a. The data, however, do not indicate this. The major formation of hydrogen bonds is likely to take place between the polymer chains. Thus SPIII probably interacts primarily with the end groups of NY-4 (Figure 9c)

Table II
 E_a^R ($\text{kJ}\cdot\text{mol}^{-1}$)

	NY-4	NY-6-(2D)	NY-6(ND)	NY-11	NY-12
SPI					
"low"	5.7 ± 0.2	5.3 ± 0.3	4.9 ± 0.3	6.1 ± 0.4	6.3 ± 0.2
"medium"	21.8 ± 1.0	27 ± 2	22.5 ± 1.6	19.6 ± 1.2	14.1 ± 1.1
"high"	66 ± 3	59 ± 4	59.5 ± 1.7	63.2 ± 1.9	60.9 ± 1.9
SPII					
"low"	8.0 ± 0.3	6.13 ± 0.18	6.38 ± 0.13	5.76 ± 0.11	5.73 ± 0.12
"high"	53 ± 3	56 ± 3	57 ± 4	66 ± 3	65.4 ± 1.2
SPIII					
"low"	7.9 ± 0.4	6.8 ± 0.3	6.77 ± 0.09	6.6 ± 0.3	5.69 ± 0.13
"medium"	26.1 ± 1.2	47.5 ± 1.3	35.5 ± 0.9	32 ± 2	26 ± 2
"high"			53.2 ± 1.7	68 ± 3	73 ± 4

and rotates more easily. The results for SPI can be interpreted in the same way as SPIII; i.e., the behavior of E_a^R for SPI in the "medium"-temperature region reflects the interaction between the amide group of SPI and the nylon chain. It is concluded that both the methylene chain length and the drawing process affect the rotation around the single bond mainly through the interaction effects.

E_a^R in the temperature region above T_n ("high") was almost constant for SPI. For SPII and SPIII, it increased with increasing methylene chain length. Here it should be considered that the activation energy of diffusion is affected by a jumping distance and a barrier height. In the "high"-temperature region the probe molecule rotates together with translational diffusion. The molecular motion of the nylon becomes greater with the number of methylene groups, and the jumping distance becomes larger. The greater the jumping distance, the greater is the segmental volume of polymer associated with the local motions. The increase of the jumping distance, and of the barrier height, results in an increase of E_a^R . The barrier height presumably increases with increasing molar volume of the spin probe. For NY-4, NY-6(2D), and NY-6(ND), the barrier effect is predominant and thus E_a^R decreases in the order SPI > SPII > SPIII. On the other hand, the barrier effect does not appear for NY-11 and NY-12, and E_a^R increases in the order SPI < SPII < SPIII because the smaller probe molecule gives the larger jumping distance. From the above argument we can conclude that the rotation of the whole probe molecule is strongly correlated with the translational diffusion of the spin probe.

Here it is worthwhile to note that for SPIII, E_a^R in the "high"-temperature region for NY-6(ND) ($53.2 \text{ kJ}\cdot\text{mol}^{-1}$) is similar to E_a^R in the "medium"-temperature region for NY-6(2D) ($47.5 \text{ kJ}\cdot\text{mol}^{-1}$). As E_a^R in the "high"-temperature region is not affected by the drawing of the nylon film, E_a^R in this region for NY-6(2D) can be assumed as $53.2 \text{ kJ}\cdot\text{mol}^{-1}$. This fact suggests that for NY-6(2D), E_a^R 's in the "high"- and "medium"-temperature region are similar so that the crossover point T_n was not detected. On the other hand, T_n of NY-4 exists in a higher temperature region than the temperature range examined in the present work because τ_R at T_n is $(3-4) \times 10^{-9} \text{ s}$ and τ_R of NY-4 does not reach this value. Thus the assignment of the mode of the rotational motion to the temperature region is reasonable.

Anisotropy of Rotation. The anisotropy of the rota-

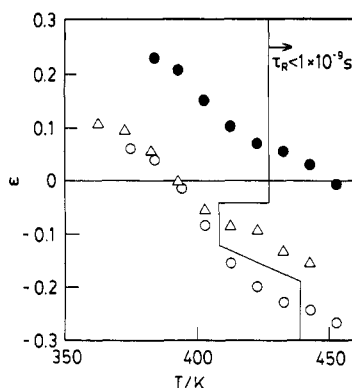


Figure 10. ϵ vs. temperature. NY-12. (O) SPI; (●) SPII; (Δ) SPIII.

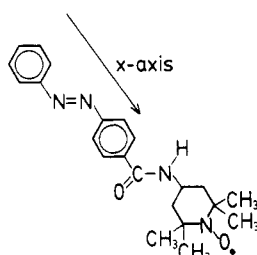


Figure 11. Rotational axis of SPI.

tion has been correlated to anisotropy parameters ϵ and δ .^{25,26}

$$\epsilon = (R_+ - 1)/(R_- - 1) \quad (3)$$

$$\delta = (R_+ + R_- - 2)/(R_+ - R_-) \quad (4)$$

In isotropic rotation, ϵ equals zero and $|\delta|$ is unity. In the region from 1×10^{-9} to 5×10^{-9} s of τ_R , however, the premises with which eq 1 was derived are not necessarily fulfilled, and ϵ and $|\delta|$ reflect not only the anisotropy but also the mobility of the probe molecules. The mobility effect makes ϵ and $|\delta|$ larger than zero and unity, respectively. As ϵ and $|\delta|$ behave in the same way, ϵ is used in this discussion. The behavior of ϵ does not vary in different nylons, so the results for NY-12 are discussed because the smallest τ_R was measured in all the nylons. Figure 10 shows that the behavior of ϵ varies from probe to probe. For SPI and SPIII, ϵ is less than zero even in the region $\tau_R > 1 \times 10^{-9}$, indicating clearly that they rotate anisotropically about the x axis,²⁷ which corresponds to the N-O bond direction, even if the mobility effect is considered in this region. As shown in Figure 11, the long axis of SPI corresponds to the x axis and the molecule rotates most easily around this axis. The single bond of SPI and SPIII also corresponds to the x axis, supporting the idea that rotation around the single bond occurs. ϵ for SPIII is closer to zero than for SPI, indicating that the rotation of SPIII is less anisotropic than for SPI. On the other hand, for SPII, τ_R becomes less than 1×10^{-9} s only in the temperature range above 433 K. In this region ϵ for SPII is almost zero and thus the probe rotates almost isotropically. Thus the structure of the spin probe greatly influences the anisotropy of rotation. τ_R as used in the present work is calculated without considering the anisotropy. Recently τ_R has been calculated with consideration of the anisotropy,^{28,29} and E_a^R so determined is comparable to the "apparent activation energy" obtained assuming isotropic rotation. This suggests that the above discussion is reasonable.

Conclusion

The mobility of the spin probes is influenced by the structure of the probe molecules, by the structure of the macromolecules, and by the interaction between the probe molecules and the macromolecules. Spin probes having an amino or amide group interact with the amide and end groups of the nylon, leading to large effects on the mobility. Thus the location of the spin probe in the polymer varies from probe to probe, and the hydrophobic spin probe SPII presumably locates near the methylene chain. This is suggested by the effects of water in NY-6(2D).¹⁷ A hydrophilic spin probe is more easily influenced by water than a hydrophobic one. As water locates in the hydrophilic part of the nylon, SPI and SPIII are believed to locate primarily in the same region.

The mobility of the spin probes increased with an increase in the number of methylene groups, reflecting the mobility of the nylon chain. The rotational activation energies in the "high"-temperature region were governed by the jumping distance and the barrier height. Effects of drawing were observed in the "medium"-temperature region, and it is concluded that the orientation of the polymer chain affects the interaction of the spin probe with the polymer. From the above results we can conclude that the specific interactions between the probe molecules and the macromolecules should be considered, as it has an important role in modifying the molecular motions of the probe molecules.

Acknowledgment. We express hearty thanks to Prof. Dr. Hiroshi Tomiyasu and Dr. Masayuki Harada of Research Laboratory for Nuclear Reactors, Tokyo Institute of Technology, for ESR measurements.

Registry No. SPI, 92412-48-1; SPII, 14565-61-8; SPIII, 14691-88-4; nylon 4 (SRU), 24938-56-5; nylon 6 (SRU), 25038-54-4; nylon 11 (SRU), 25035-04-5; nylon 12 (SRU), 24937-16-4; poly-(2-pyrrolidinone), 24968-97-6; poly(11-aminoundecanoic acid), 25587-80-8; poly(azacyclotridecan-2-one), 25038-74-8.

References and Notes

- (1) Boyer, R. F.; Keimath, S. E., Eds. *Molecular Motion in Polymers by ESR*; Harwood Academic: New York, 1980.
- (2) Berliner, L. J., Ed. *Spin Labeling. Theory and Applications*; Academic: New York, 1976, Vol. 1; 1979, Vol. 2.
- (3) Kumler, P. L. *Methods Exp. Phys.* **1980**, *16A*, 442.
- (4) Kumler, P. L.; Boyer, R. F. *Macromolecules* **1976**, *9*, 903.
- (5) Braun, B.; Törmälä, P.; Weber, G. *Polymer* **1978**, *19*, 598.
- (6) Törmälä, P.; Weber, G. *Polymer* **1978**, *19*, 1026.
- (7) Kusumoto, N.; Sano, S.; Zaitzu, N.; Motozato, Y. *Polymer* **1976**, *17*, 448.
- (8) Bullock, A. T.; Cameron, G. G.; Miles, I. S. *Polymer* **1982**, *23*, 1536.
- (9) Bueche, F., Ed. *Physical Properties of Polymers*; Wiley-Interscience: New York, 1962.
- (10) Kusumoto, N.; Yonezawa, M.; Motozato, Y. *Polymer* **1974**, *15*, 793.
- (11) Meirovitch, E. *J. Phys. Chem.* **1984**, *88*, 2629.
- (12) Choy, C. L.; Leung, W. P.; Ma, T. L. *J. Polym. Sci., Polym. Phys. Ed.* **1985**, *23*, 557.
- (13) Kaifu, K.; Komai, T.; Tsutsumi, A. *Polym. J.* **1982**, *14*, 803.
- (14) Komai, T.; Yano, E.; Kawasaki, T.; Hashizume, S. *Polym. J.* **1984**, *16*, 317.
- (15) Törmälä, P.; Penttilä, T.; Lindberg, J. J.; Sundquist, J. *Finn. Chem. Lett.* **1976**, 170.
- (16) Törmälä, P. *Colloid Polym. Sci.* **1977**, *255*, 209.
- (17) Hamada, K.; Iijima, T.; McGregor, R. *Polym. J.* **1985**, *17*, 1245.
- (18) McGregor, R.; Iijima, T.; Sakai, T.; Gilbert, R. D.; Hamada, K. *J. Membr. Sci.* **1984**, *18*, 129.
- (19) Hlousková, Z.; Tinó, J.; Borsig, E. *Polym. Commun.* **1984**, *25*, 112.
- (20) Törmälä, P. *J. Macromol. Sci., Rev. Macromol. Chem.* **1979**, *C17*, 297.
- (21) Buchachenko, A. L.; Kovarskii, A. L.; Vasserman, A. M. In *Advances in Polymer Science*; Rogovin, Z. A., Ed.; Halsted (Wiley): New York, 1974; pp 26-57.
- (22) Kivelson, D. *J. Chem. Phys.* **1960**, *33*, 1094.

- (23) Kuznetsov, A. N.; Vasserman, A. M.; Volkov, A. U.; Korst, N. *N. Chem. Phys. Lett.* **1971**, *12*, 103.
 (24) Kovarskii, A. L.; Placek, J.; Szöcs, F. *Polymer* **1978**, *19*, 1137.
 (25) Kuznetsov, A. N.; Volkov, A. Y.; Livshits, V. A.; Mirzoiian, A. T. *Chem. Phys. Lett.* **1974**, *26*, 369.
 (26) Smith, P. M. *Eur. Polym. J.* **1974**, *15*, 147.
 (27) Griffith, O. H.; Jost, P. C. In *Spin Labeling. Theory and Applications*; Berliner, L. J., Ed.; Academic: New York, 1976; Vol. 1, pp 453-523.
 (28) Hwang, J. S.; Tsonis, C. P. *Macromolecules* **1983**, *16*, 736.
 (29) Shiotani, M.; Sohma, J.; Freed, J. H. *Macromolecules* **1983**, *16*, 1495.

Spectroscopic Study of the Photodegradation Pathways of Silver-Backed Polyacrylonitrile Films

C. A. Sergides, A. R. Chughtai, and D. M. Smith*

Department of Chemistry, University of Denver, Denver, Colorado 80208

P. Schissel

Solar Energy Research Institute, Golden, Colorado 80401. Received October 18, 1985

ABSTRACT: Ultraviolet radiation in the regions $266 \leq \lambda \leq 400$ nm and $250 \leq \lambda \leq 400$ nm has been employed to study the oxidative photodegradation pathways for silver-backed polyacrylonitrile film. Measurements based on Fourier transform infrared reflection absorbance (FTIR-RA) spectroscopy were supported by electron paramagnetic resonance (EPR) studies. Isotopic ^{13}C PAN was used to confirm some photodegradation products. Upon irradiation at wavelengths below 266 nm the polymer turns yellowish-brown and also increases in electrical conductivity, suggesting the presence of a chromophore system of the type $(>\text{C}=\text{N}-)_n$.

Introduction

Protective films have been used recently for photovoltaic solar energy conversion systems.¹⁻³ In particular, polymers have been applied to protect metallic surfaces from exposure to environmental degradation.⁴⁻⁸ The photodegradation of the polymeric films remains an obstacle and the selection of the photostabilizers and photoinhibitors⁹ is extremely dependent on the type of degradation, e.g., oxidative or nonoxidative. Therefore, an understanding of the photodegradation mechanisms of aluminum- or silver-backed polyacrylonitrile (PAN) films is important for their effective utilization in solar energy systems. There have been numerous studies of the thermal degradation and the mechanism of color formation in PAN (solid or liquid), of which several recent publications¹⁰⁻¹⁵ are representative. However, there are a limited number of investigations^{16,17} of the UV photodegradation of this polymer. Burlant et al.¹⁸ studied the effect of high-energy radiation (1-meV electrons) on PAN films in the presence and absence of oxygen. But a fundamental and systematic study of the photodegradation of PAN/Ag films in the $250 \leq \lambda \leq 400$ -nm region of the spectrum has yet to be accomplished. Fourier transform infrared reflection absorption (FTIR-RA) spectroscopy is a useful tool for obtaining analytical information on surface reactions. The technique is sensitive, reproducible, and nondestructive with high signal-to-noise (S/N) ratios achievable and with computer software enabling the digital subtraction of spectra. Several authors have used recently an FTIR technique to study the thermal degradation of PAN under vacuum, oxidative, and nonoxidative environments.¹⁹⁻²¹

Experimental Section

The spectrophotometer used for these experiments is a Digilab FTS-14B equipped with mercury cadmium telluride (MCT) and triglycine sulfate (TGS) detectors. Two controlled environment chambers were designed to fit the spectrometer sample compartment as shown in Figure 1. An earlier chamber^{4,22} used to collect the infrared spectra of polymeric coatings on mirrors, while simultaneously undergoing exposure to UV and flowing ambient gases (e.g., O_2 , N_2), was modified by attaching two thermistors, one on the film and the other on the reference mirror, to record

the temperature achieved during the UV exposure. The second chamber²³ is vacuum tight and can be used to study both the degradative changes in the film as well as the gases produced during UV irradiation. These chambers were designed to maximize the sensitivity of the absorbing species to IR (the angle of incidence was kept at 78°).²⁴⁻²⁶ The irradiation of the PAN/Ag film was accomplished through the quartz windows of the chambers by an SS-1000-2 solar simulator supplied by the Optical Radiation Co. (ORC). For these experiments, UV light with $266 \leq \lambda \leq 400$ nm (dichroic filter) at air mass one and $250 \leq \lambda \leq 400$ nm (without dichroic filter) were used. The spectral distribution of the ORC simulator at air mass one and without dichroic filter is given in Figure 2. The acrylonitrile polymer with an average molecular weight of 150 000 and intrinsic viscosity of 1.95 dL g^{-1} was obtained from E. I. duPont de Nemours and Co.

Experiments on the solubility of PAN in various solvents indicated dimethyl sulfoxide (Me_2SO) to be the most suitable solvent to yield thin films. Clear films of PAN, of approximately $4.4\text{-}\mu\text{m}$ thickness, were successfully drawn at a rate of 1 mm s^{-1} in nitrogen. The optimum concentration of PAN in Me_2SO was about 8% (w/v). The PAN-coated mirrors were dried in nitrogen and then in a vacuum oven at 72°C for 48 h. The IR-RA spectra (Figure 3) of these films were consistent with the reference spectra of PAN²⁷⁻²⁹ and our own spectra of the polymer. (It should be remembered that the relative intensities of absorption bands are dependent upon film orientation). There was no spectroscopic evidence for entrapped Me_2SO solvent in these films. As indicated by their IR spectra, the Ag-supported PAN films were of a very satisfactory quality for the study of polymer degradations. The irradiation of PAN was carried out under both oxidative conditions (dry purge air, oxygen-16, and oxygen-18) and a nonoxidative atmosphere (N_2) in both chambers described earlier. The flow rate of gases in the open chamber was maintained at $40 \text{ cm}^3 \text{ s}^{-1}$. After stabilization of the xenon lamp for 25 min, the sample was exposed to UV radiation for a specific time. The IR spectra were collected during and after the period of exposure. The loss of the original bands in the polymer and the formation of new bands during the photodegradation were studied from the absorbance subtraction spectra. The maximum temperature reached during the irradiation of PAN/Ag samples as measured by the thermistors was 57°C .

Results and Discussion

The PAN/Ag film was exposed to UV light of $266 \leq \lambda \leq 400$ nm (dichroic filter at air mass 1, Figure 2) for as long